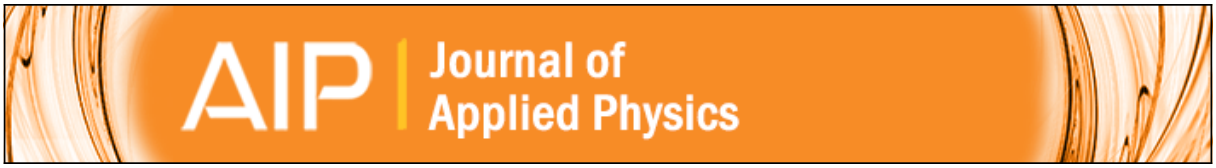

Infraredabsorption spectra associated to transitions from donor states to conduction subbands in GaAs(Ga,Al)As quantum wells

J. Sabin del Valle, M. de DiosLeyva, and L. E. Oliveira

Citation: Journal of Applied Physics **80**, 1142 (1996); doi: 10.1063/1.362851

View online: http://dx.doi.org/10.1063/1.362851

View Table of Contents: http://scitation.aip.org/content/aip/journal/jap/80/2?ver=pdfcov

Published by the AIP Publishing

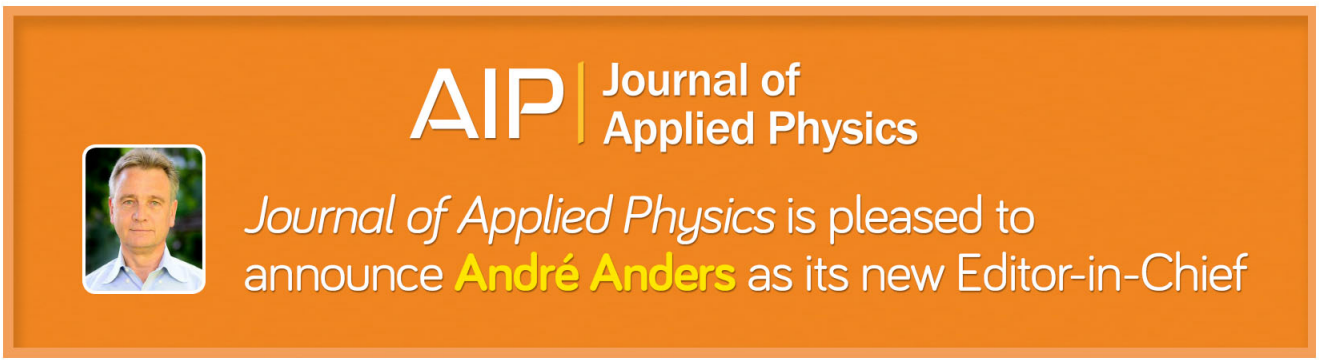

Infrared-absorption spectra associated to transitions from donor states to conduction subbands in GaAs-(Ga,Al)As quantum wells

J. Sabin del Valle[a)]
Instituto de Física, Universidade Estadual de Campinas—Unicamp, Caixa Postal 6165, Campinas, São Paulo, 13083-970, Brazil

M. de Dios-Leyva
Departamento de Física Teórica, Universidad de La Habana, San Lázaro y L, Vedado, Havana, Cuba

L. E. Oliveira[b)]
Instituto de Física, Universidade Estadual de Campinas—Unicamp, Caixa Postal 6165, Campinas, São Paulo, 13083-970, Brazil

(Received 4 December 1995, accepted for publication 12 March 1996)

The infrared-absorption spectra associated with transitions from donor states to conduction subbands in GaAs–(Ga,Al)As quantum wells are systematically studied. The absorption spectra are calculated within the effective-mass approximation and with a variational procedure for evaluating donor energies and envelope wave functions. Calculations are presented for incident radiation polarized both in the growth direction and in the plane perpendicular to it. Theoretical results are analyzed for different quantum-well widths and $n=1,2$ conduction subbands, and compared with available experimental measurements. © *1996 American Institute of Physics.* [S0021-8979(96)01112-7]

I. INTRODUCTION

In the past years there has been a considerable interest in the physical properties associated with semiconductor superlattices and heterostructures.[1] This is connected with the potential device applications of these systems.[2–4] One of the aspects of fundamental interest is the study of impurity states associated with semiconducting heterostructures. Bastard[5] was the first to study the properties of shallow hydrogenic impurities in quantum wells (QWs). He considered an infinite QW and studied the optical-absorption spectra associated with transitions involving valence subband → ''donor-impurity band'' and ''acceptor-impurity band'' → conduction subband. His work was followed by more detailed investigations.[6–10] Greene and Bajaj[6] studied the energies of the ground state and a few excited impurity states taking into account the finite barrier at the GaAs QW interfaces, whereas Mailhiot, Chang, and McGill[7] considered both the effects of the dielectric-constant and effective-mass mismatches at the interfaces. Tanaka, Nagaoka, and Yamabe[8] considered impurity states in finite QWs with asymmetric barriers, and Masselink, Chang, and Morkoç studied the effect of the complex valence-band structure on the shallow acceptor states in GaAs–(Ga,Al)As QWs. Oliveira and Pérez-Alvarez[10] analyzed the optical-absorption spectra associated with shallow impurities in GaAs–(Ga,Al)As QWs. Experimentally, the observation of acceptor-related features in the photoluminescence spectra of GaAs–(Ga,Al)As QWs was reported by Miller *et al.*,[11] and properties of donors in those QWs have been studied by Shanabrook *et al.*[12,13] (see also the reviews on the subject[14–16]). Oliveira and López-Gondar[17] theoretically studied the acceptor-related photoluminescence spectra of GaAs–(Ga,Al)As QWs, whereas Oliveira and de Dios-Leyva[18] considered the effects of shallow acceptors in the QW photoluminescence process under steady-state excitation conditions, and calculated carrier densities, electron and hole quasi-Fermi levels, and various radiative decay lifetimes as functions of the cw laser intensity, well widths, temperature, and acceptor distribution in the well. Although there is quite a considerable amount of experimental and theoretical work on hydrogenic impurities in QWs, there are still some theoretical aspects to be considered, and experimental work is not complete.

II. THEORY

The present work is concerned with the infrared-absorption spectra associated with transitions between the donor-impurity band and the conduction subbands for a GaAs–$Ga_{1-x}Al_xAs$ QW. We assume that the temperature is low enough ($T \ll 100$ K) such that each donor state is filled with an electron. The Hamiltonian of a shallow hydrogenic donor in a GaAs layer sandwiched between two semi-infinite slabs of GaAs–$Ga_{1-x}Al_xAs$ may be written, in the effective-mass approximation, as

$$H=-\frac{\hbar^2\nabla^2}{2m^*}-\frac{e^2}{\epsilon_0[\rho^2+(z-z_i)^2]^{1/2}}+V(z), \tag{1}$$

in which the barrier potential $V(z)$ is taken to be a square well of height V_b and width L. The size V_b of the barrier is taken to be 60% of the band-gap discontinuity, ΔE_g (eV)$=1.247x$, in the GaAs–$Ga_{1-x}Al_xAs$ heterostructure for the conduction band.[19,20] In Eq. (1) z_i is the position of the impurity with respect to the $z=0$ origin chosen at the center of the well, $r=[\rho^2+(z-z_i)^2]^{1/2}$, with $\rho=(x^2+y^2)^{1/2}$, is the distance from the carrier to the impurity site, $\epsilon_0=12.35$ is the static

[a)]On sabbatical leave from Departamento de Física, Instituto Superior Pedagógico Enrique José Varona, Ciudad Libertad, Marianao, Habana 11400, Cuba.
[b)]Electronic mail: oliveira@ifi.unicamp.br

 0021-8979/96/80(2)/1142/4/$10.00

dielectric constant, $m^*=0.0665m_0$ is the effective mass (we assume the values of the dielectric constant and effective mass to be the same as in GaAs for all regions of the heterostructure), and m_0 is the free electron mass. In calculating the donor energies we use a variational procedure and an impurity trial wave function which is allowed to penetrate into the $Ga_{1-x}Al_xAs$ barriers, i.e., we use as the donor ground-state envelope wave function a simple one-parameter variational $1s$-hydrogeniclike wave function times the ground-state $g_1(z)$ solution for the QW without the impurity potential,[21] and one readily obtains the donor energies and envelope wave functions, for each impurity position, by minimizing the Hamiltonian with respect to the variational parameter in the $1s$-like part of the envelope wave function. For the conduction miniband one uses the usual envelope wave function $g_n(z)\exp(i\mathbf{k}_\perp\cdot\rho)$ [$g_n(z)$ is the solution for the QW without the impurity potential], where n is the quantum number associated to the specific conduction miniband in consideration.

For a single impurity located at $z=z_i$, the transition probability per unit time for the donor state $\rightarrow$ conduction miniband transition is proportional to the square of the matrix element of the electron–photon[22] interaction between the wave functions of the initial (donor) and the final (conduction) states,

$$W_L(z_i,\omega)=\frac{2\pi}{\hbar}\left(\frac{eA_0}{m^*c}\right)^2\sum_{\mathbf{k}_\perp,s}|\langle f|\mathbf{e}\cdot\mathbf{p}|i\rangle|^2\delta(E_f-E_i-\hbar\omega), \tag{2}$$

where s means summation over spin, $\mathbf{e}$ is the polarization vector in the direction of the electric field of the radiation, $\mathbf{p}$ is the momentum operator, A_0 is the photon vector potential, and the other symbols have their usual meaning. For a $GaAs–Ga_{1-x}Al_xAs$ QW of width L, the transition probability per unit time (associated with a single impurity located at $z=z_i$) for the donor $\rightarrow n=1$ conduction subband is therefore given by

$$W_L(z_i,\omega)=W_0\left.\frac{N^2(N_b^0)^2(J^0)^2}{(m^*/m_0)}\right|_{\mathbf{k}_\perp(\omega)}Y[\Delta^0(\omega)], \tag{3}$$

where $Y(x)$ is the step function, $N=(1/\langle\psi|\psi\rangle)^{1/2}$ is the normalization factor for the impurity wave function, and N_b^0 is the normalization factor for the wave function associated with the first conduction subband. In Eq. (3)

$$\Delta^0(\omega)=\hbar\omega-E(L,z_i), \tag{4a}$$

$$k_\perp(\omega)=[2m^*\Delta^0(\omega)/\hbar^2]^{1/2}, \tag{4b}$$

$$W_0=e^2A_0^2/\hbar m_0c^2, \tag{4c}$$

where $E(L,z_i)$ is the donor binding energy. For $J^0=J^0[z_i,\lambda,k_\perp(\omega)]$ in Eq. (3), we have

$$J^0=(e_x^2+e_y^2)(J_1^0)^2+2e_z^2(J_2^0)^2, \tag{5}$$

where λ is the impurity-wave function variational parameter, e_x, e_y, and e_z are the components of the polarization vector $\mathbf{e}$, and J_1^0 and J_2^0 are cumbersome functions of z_i,λ, $k_\perp(\omega)$, and of the QW width L. In the case of transitions from the donor-impurity band $\rightarrow n=2$ conduction subband, a similar expression to Eq. (3) may be obtained.

For the case of a donor located at the center of the QW, an analysis for the donor $\rightarrow n=1$ conduction subband transitions using the expressions for J_1^0 and J_2^0 in Eqs. (3)–(5) (or similar equations for the donor $\rightarrow n=2$ conduction subband transitions) shows that for an incident radiation with polarization $e_x\neq0$ and/or $e_y\neq0$, with $e_z=0$, the transition is allowed (forbidden), whereas for $e_x=e_y=0$, with $e_z\neq0$, it is forbidden (allowed).

Finally, we consider the total transition probability per unit time, for a distribution of impurities $P(z_i)$ inside the QW, and we have

$$W(\omega)=\int_{-L/2}^{L/2}dz_i\ P(z_i)W_L(z_i,\omega). \tag{6}$$

III. RESULTS AND DISCUSSION

To carry out the numerical calculations, we considered a 30% Al concentration in the barrier, and both the cases in which the polarization vector of the electric field of the incident radiation is either in the plane perpendicular to the z growth axis (i.e., $e_z=0$), or the incident radiation is polarized along the z axis ($e_z=1$). For simplicity, we have assumed an homogeneous distribution of impurities [i.e., $P(z_i)=1/L$ in Eq. (6)] within the QW.

Figure 1(a) shows the $e_z=0$ infrared-absorption spectrum $W(\omega)$ (in units of W_0) corresponding to donor-to-ground conduction subband transitions for a homogeneous distribution of donors in an $L=10$ nm $GaAs–Ga_{0.7}Al_{0.3}As$ QW (solid curve). Also, the contributions $W(z_i,\omega)$ are shown for two different impurity positions, on edge (dotted curve) and on center (dashed curve). As expected, there is no absorption for $\hbar\omega<E(L,z_i)$. A comparison of the absorption spectra associated with transitions from the donors to the $n=1$ conduction subband (solid curve) and to the $n=2$ conduction subband (dashed curve) for a $L=10$ nm $GaAs–Ga_{0.7}Al_{0.3}As$ QW is presented in Fig. 1(b). It is apparent that the absorption for transitions to the $n=2$ conduction subband is very weak in comparison to the absorption for transitions to the $n=1$ subband. This is due to the poor overlapping of the wave functions of the donor states with the $n=2$ subband states in comparison with the overlap with electron states associated to the $n=1$ conduction subband.

In Fig. 2 the $e_z=0$ infrared-absorption spectra $W(\omega)$ (in units of W_0) are shown for donor-to-ground conduction subband transitions, and $GaAs–Ga_{0.7}Al_{0.3}As$ QWs of different widths. Note that the narrower the QW, the higher the value for the absorption peak obtained, and that the energy corresponding to this maximum as well as the threshold energy increase. This behavior shows, for example, the importance of using narrow QWs for stronger absorption.

Finally, Fig. 3 shows the $e_z=1$ infrared-absorption spectra associated to transitions from the donor-impurity band to the $n=1$ conduction subband considering an homogeneous donor distribution within the $L=40$ nm $GaAs–Ga_{0.7}Al_{0.3}As$ QW. The theoretical results are in good agreement with the 63 cm^{-1} peak of the absorption spectrum measured by Helm

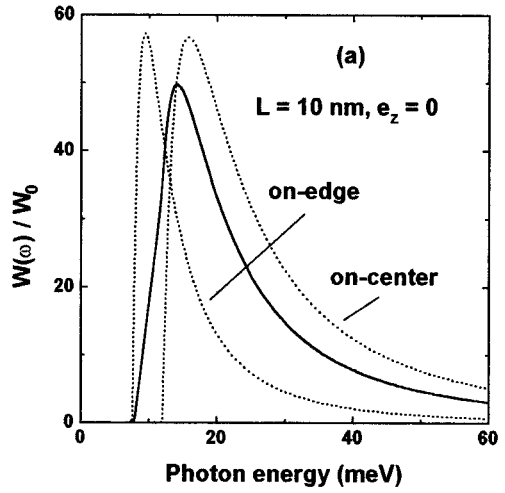

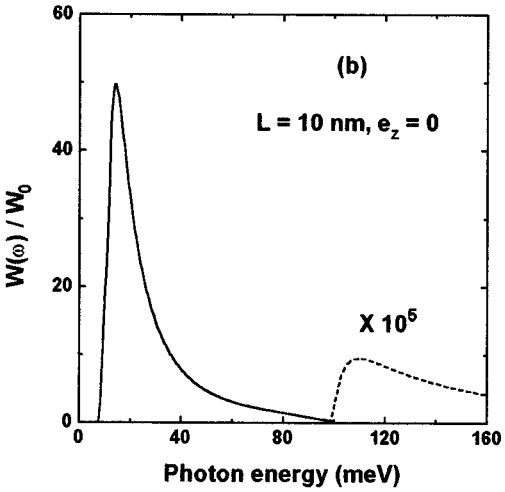

FIG. 1. (a) Infrared-absorption spectrum (in units of W_0) for transitions from the donor impurity band to the ground conduction subband for a $L=10$ nm GaAs–$Ga_{0.7}Al_{0.3}As$ QW doped with an homogeneous distribution of impurities (solid curve). The dotted curves correspond to the absorption contribution due to on-edge and on-center donors. (b) Absorption spectra (in units of W_0) for transitions from the donor impurity band to the $n=1$ conduction subband (solid curve) and to the $n=2$ first excited subband (dashed curve) for a $L=10$ nm GaAs–$Ga_{0.7}Al_{0.3}As$ QW. For both (a) and (b) the incident radiation has $e_z=0$ in-plane polarization, i.e., the polarization is in the plane perpendicular to the growth axis.

et al.,[23] which was then assigned to transitions involving the conduction minibands $n=1$ and $n=2$. We believe our theoretical results in Fig. 3 (valid at low temperatures, $T \ll 100$ K) indicate that the experimental feature around 63 $cm^{-1} \approx 7.8$ meV, observed by Helm *et al.*[23] at $T=6$ K (see Fig. 5 of Ref. 23) corresponds essentially to transitions from the ground-state $1s$-like donor states to the $n=1$ conduction miniband, and as the temperature increases (see experimental data at $T=20$ K and $T=60$ K), the donors become ionized, the $n=1$ conduction subband becomes occupied, and the $n=1 \rightarrow n=2$ conduction transitions are then dominant.

It is important to note that, in contrast to bulk diluted-doped materials, where the donor level is a sharp and discrete one, those infrared-absorption spectra from donor-impurity band to conduction subbands provide some information on the width of the donor-impurity band in GaAs–(Ga,Al)As QWs, as donor levels may strongly depend on the impurity position. Also, as we are treating donors in GaAs–(Ga,Al)As QWs, we have used the standard parabolic-band model in the effective-mass approximation (which has proved to be adequate in a number of physical situations of donors in QWs) in order to obtain the impurity energy levels and envelope wave functions within a variational procedure. Of course, if one is interested in treating the similar acceptor problem, the complex structure of the valence band must be taken into account for a realistic description of the acceptor-related infrared absorption.

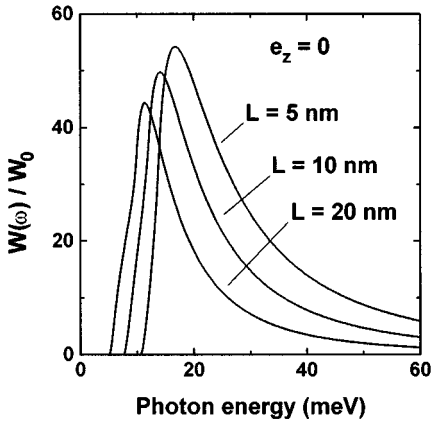

FIG. 2. Infrared absorption spectra (in units of W_0) for transitions from the donor impurity band to the $n=1$ conduction subband for GaAs–$Ga_{0.7}Al_{0.3}As$ QWs of different widths and doped with an homogeneous distribution of impurities. The incident radiation has $e_z=0$ in-plane polarization, i.e., the polarization is in the plane perpendicular to the growth axis.

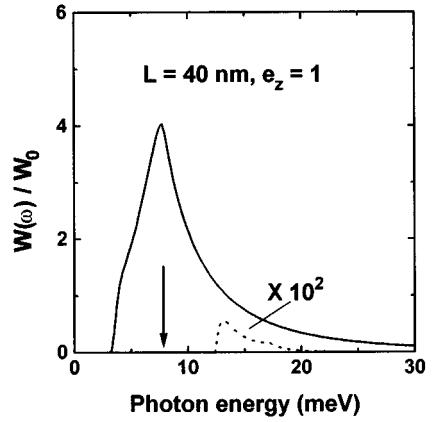

FIG. 3. Infrared-absorption spectra (in units of W_0) for transitions from the donor impurity band to the $n=1$ conduction subband (solid curve) and to the $n=2$ first excited subband (dashed curve) for an $L=40$ nm GaAs–$Ga_{0.7}Al_{0.3}As$ QW doped with an homogeneous distribution of impurities. The incident radiation is polarized along the growth axis, i.e., $e_z=1$. The arrow in the horizontal axis corresponds to a peak in the experimental results of Helm *et al.* (see Ref. 23).

IV. CONCLUSION

In conclusion, we have analytically calculated the infrared-absorption spectra associated with transitions from the donor impurity band to the two lowest conduction subbands. Also, we have studied in some detail the total transition probability per unit time considering a range of quantum-well widths, transitions to different conduction subbands, and different polarizations of the incident radiation. Although experimental data for a systematic comparison with our theoretical results are still incomplete, we believe the present study would be of help in the quantitative understanding of future experimental work in the area.

ACKNOWLEDGMENTS

This work was partially supported by Brazilian Agencies CNPq, FAPESP, FINEP, and FAEP-UNICAMP.

[1] L. Esaki, in *Recent Topics in Semiconductor Physics*, edited by H. Kamimura and Y. Toyozawa (World Scientific, Singapore, 1983), p. 1.
[2] J. P. van der Ziel, R. Dingle, R. C. Miller, W. Wiegmann, and W. A. Nordland, Jr., Appl. Phys. Lett. **26**, 463 (1975).
[3] R. Dingle, H. L. Stormer, A. C. Gossard, and W. Wiegmann, Appl. Phys. Lett. **33**, 665 (1978).
[4] J. N. Schulman and T. C. McGill, Appl. Phys. Lett. **34**, 663 (1979).
[5] G. Bastard, Phys. Rev. B **24**, 4714 (1981).
[6] R. L. Greene and K. K. Bajaj, Solid State Commun. **45**, 825 (1983).
[7] C. Mailhiot, Y.-C. Chang, and T. C. McGill, Phys. Rev. B **26**, 4449 (1982).
[8] K. Tanaka, M. Nagaoka, and T. Yamabe, Phys. Rev. B **28**, 7068 (1983).
[9] W. T. Masselink, Y.-C. Chang, and H. Morkoç, Phys. Rev. B **28**, 7373 (1983).
[10] L. E. Oliveira and R. Pérez-Alvarez, Solid State Commun. **70**, 523 (1989); Phys. Rev. B **40**, 10 460 (1989).
[11] R. C. Miller, A. C. Gossard, W. T. Tsang, and O. Munteanu, Phys. Rev. B **25**, 3871 (1982).
[12] B. V. Shanabrook and J. Comas, Surf. Sci. **142**, 504 (1984).
[13] B. V. Shanabrook, J. Comas, T. A. Perry, and R. Merlin, Phys. Rev. B **29**, 7096 (1984).
[14] R. L. Greene and K. K. Bajaj, Solid State Commun. **53**, 1103 (1985).
[15] G. Bastard, J. Lumin. **30**, 488 (1985).
[16] C. Delalande, Physica B–C **146B**, 112 (1987); B. V. Shanabrook, *ibid*. **146B**, 121 (1987); Y.-C. Chang, *ibid*. **146B**, 137 (1987).
[17] L. E. Oliveira and J. López-Gondar, Phys. Rev. B **41**, 3719 (1990).
[18] L. E. Oliveira and M. de Dios-Leyva, Phys. Rev. B **48**, 15 092 (1993).
[19] R. C. Miller, D. A. Kleinman, and A. C. Gossard, Phys. Rev. B **29**, 7085 (1984).
[20] W. Wang, E. E. Mendez, and F. Stern, Appl. Phys. Lett. **45**, 639 (1984).
[21] L. E. Oliveira, Phys. Rev. B **38**, 10 641 (1988); Superlattices and Microstructures **5**, 23 (1989).
[22] F. Bassani and G. Pastori Parravicini, in *Electronic States and Optical Transitions in Solids*, edited by R. A. Ballinger (Pergamon, Oxford, 1975).
[23] M. Helm, F. M. Peeters, F. DeRosa, E. Colas, J. P. Harbison, and L. T. Florez, Phys. Rev. B **43**, 13 983 (1991).